Fractal dimension of scattering equivalent section of aerosol and its calibration mechanism

Fang Gu (顾 芳)[1*], Jiahong Zhang (张加宏)[2], and Yulin Chen (陈玉林)[1]

[1] *College of Math & Physics, Nanjing University of Information Science & Technology, Nanjing 210044, China*

[2] *College of Electronic & Information Engineering, Nanjing University of Information Science & Technology, Nanjing 210044, China*

[*] *E-mail: gfnuist@yahoo.cn*

Received February 18, 2009

The correct calibration of coefficients in the inversion model for aerosol mass concentration is the precondition of obtaining highly precise results. The concept of the fractal dimension of scattering equivalent section is presented, and the calibration mechanism of the fractal dimension is discussed. Based on the calibration mechanism, the stability of the fractal dimension is analyzed. Theoretical analysis and experimental results indicate that the fractal dimension obtained by the intersection point calibration method is stable, while that calibrated by the Gauss-Newton method is instable, which only describes the shape characteristic of a small sample. The study of the calibration mechanism for the fractal dimension markedly enhances the present model for aerosol mass concentration.

OCIS codes: 290.5850, 120.5820, 010.1100.

doi: 10.3788/COL20090709.0857.

Environment pollution has been growing into a serious problem in the world, and aerosol plays an important adverse role in the atmosphere, affecting global climate and reducing atmospheric visibility[1]. There is also an evidence that aerosol can have a negative effect on human health[2]. Hence, how to measure aerosol mass and number concentration has generated considerable interest. Recently, in order to realize simultaneous measurement of aerosol number and mass concentrations, the single particle scattering technique that is usually used to measure number concentration is gradually abopted to detect mass concentration. However, there are only a few products using this technique which can measure mass concentration till now[3]. Based on a detailed theoretical analysis, we have proposed a systemic model for aerosol mass concentration by the single particle scattering technique[4−6], which takes the particle-shape effect into consideration and overcomes the difficult problem of calibration in the case of large number of channels compared with the existing model[3,7]. In this letter, in order to make the physical meaning of the model clearer, the concept of the fractal dimension of scattering equivalent section is put forward, and the calibration mechanism of the coefficients in our model is carefully investigated.

According to the Mie theory, the formula for mass concentration of spherical particles with an optical particle counter (OPC) under the condition of a uniform intensity distribution in optical sensing volume is derived as[4]

$$C_s = k_s \sum_{i=1}^{q} s(v_i) v_i^{1.5}, \tag{1}$$

where k_s is the proportional coefficient, which has the same dimension with mass concentration; v_i is the relative median voltage in the ith channel of an OPC; q is the number of channels; $s(v_i)$ is the pulse height distribution of spherical particles.

Based on Eq. (1), considering the nonuniform intensity distribution and irregular particles, the calculation formula for aerosol mass concentration is given by[5,6]

$$C = k \sum_{i=1}^{q} N(v_i) v_i^{\alpha}, \tag{2}$$

where k is the proportional coefficient; α is the equivalent factor; $N(v_i)$ is the pulse height distribution of irregular particles.

In Eq. (2), $N(v_i)$ can be directly measured by an OPC, and k and α are obtained by the calibration. The Gauss-Newton method (nonlinear regression) is used to calibrate k and α, but experimental results given in Table 1 show that calibration coefficients attained under different conditions are obviously different. References [8] and [9] demonstrate that environmental relative humidity (RH) has an influence on aerosols, especially when the RH is greater than 60%. But from Table 1, it can be seen that there is still a remarkable difference between these coefficients when the RH is lower than 60%. Thus there are other factors impacting the calibration of k and α. Figure 1 illustrates the relationships between the range of aerosol mass concentration, $R_{\rm C}$, and calibration coefficients, and we can see that the range of mass concentration obviously affects the coefficients. Hence, k and α calibrated by the Gauss-Newton method cannot be applied to inverse aerosol mass concentration.

Interestingly, the experimental results indicate that the calibration of α is more important than k, that is, if α is determined, and then k calculated using

$$k = \frac{1}{T} \sum_{t=1}^{T} \frac{C_{{\rm TSI},t}}{\sum\limits_{i} N_t(v_i) v_i^{\alpha}}, \tag{3}$$

is stable. In Eq. (3), T is the number of experimental

Table 1. Calibration Coefficients Calibrated by Gauss-Newton Method under Different Conditions

Date	T (°C)	RH (%)	α	$k(\times 10^{-5}$ mg/m$^3)$
2007.2.2	9.92	47.09	1.55	5.9462
2007.2.3	11.03	53.53	1.44	5.6186
2007.2.4	12.67	49.18	1.79	7.7235
2007.2.5	14.66	57.62	1.86	6.3105
2007.2.6	16.61	61.50	1.06	4.4566
2007.2.7	15.82	68.85	2.64	6.2076
2007.2.8	15.39	71.14	1.92	6.4094
2007.2.10	14.00	65.64	2.36	6.0057
2007.2.11	12.54	59.96	2.21	6.3622
2007.2.12	13.24	54.72	1.04	4.4532
2007.2.13	13.96	63.90	1.30	4.7548
2007.2.14	14.57	73.63	2.36	6.5811
2007.2.15	13.38	54.42	0.60	2.5908
Relative Standard Deviation	–	–	35%	22%

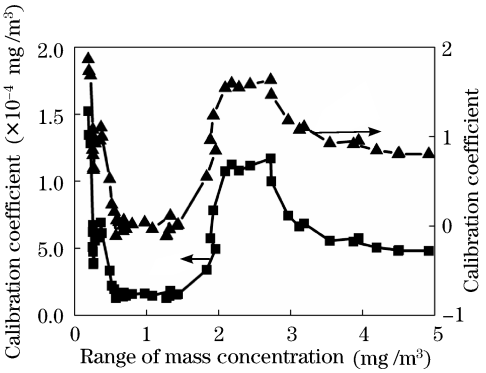

Fig. 1. Calibration coefficient as a function of the range of mass concentration.

data points, $C_{\mathrm{TSI},t}$ is the actual mass concentration at the tth measurement.

Base on the above result, the intersection point calibration method is presented to calibrate coefficients, which overcomes the instable problem of coefficients and has high inversion precision[6]. However, in our previous work, the reason of good stability and high precision of this calibration method is not given. In the following, we will discuss the physical meaning and the calibration mechanism of the equivalent factor α in our model.

As we know, the exponent 1.5 in Eq. (1) corresponds to the dimension of spherical particles, and $k_s v_i^{1.5}$ represents the mass of a spherical particle with signal voltage v_i in the case of uniform intensity distribution in optical sensing volume. Then we can deduce that if measured aerosols are regular three-dimensional (3D) particles (such as cubic particles), the exponent of v_i is also 1.5. In this way, only the proportional coefficient k_s in Eq. (1) needs to be modified to inverse mass concentration. Whereas particles existing in nature or produced by human are usually irregular particles, and many references indicate that these particles are fractal, such as soot aggregate from wood combustion and diesel, soil particles, rock particles, atmospheric aerosols, and so on[10−13]. Furthermore, Virtanen *et al.* have shown a power-law relationship between the particle mass m and the mobility equivalent diameter d_b[14]:

$$m \propto d_b^{d_{\mathrm{f}}}, \tag{4}$$

where d_{f} is the mass fractal dimension, which is a non-integer number. Therefore, the dimension of aerosol is not a 3D one. For this reason, both k_s and the exponent 1.5 in Eq. (1) need to be modified to inverse aerosol mass concentration. Because the signal voltage v_i is corresponding to the optical equivalent diameter in our model and the exponent of v_i is not 1.5, based on Eq. (4), the mass of a particle can be expressed as

$$m_i \propto v_i^{\alpha}. \tag{5}$$

Similarly, α can be considered as the fractal dimension of scattering equivalent section of aerosol, and then kv_i^{α} represents the mass of an irregular particles with signal voltage v_i. In the ith channel of an OPC, the total mass measured in a cycle is given by

$$M_i = N(v_i)(kv_i^{\alpha}). \tag{6}$$

Then the aerosol mass concentration can also be written as

$$C = \sum_{i=1}^{q} M_i = \sum_{i=1}^{q} N(v_i)(kv_i^{\alpha}). \tag{7}$$

From the above analysis, we know that the fractal dimension of scattering equivalent section, α, describes the shape characteristic of aerosol. Next, we will discuss the calibration mechanism of α on the basis of this physical meaning.

The fractal dimension α obtained by calibration experiments should describe the shape characteristic of total measured particles, not a small sample. However, only small samples can be attained in experiments. Due to differences in small samples in each range of mass concentration, the shape characteristics of these small samples are also different. In practice, it is impossible to detect aerosol over a long enough time to calibrate α, thereby, only the common shape characteristic of different small samples can be used to replace the shape characteristic of the total measured particles, which is the calibration mechanism of α. As long as α is given, k will be obtained by Eq. (3).

Based on the calibration mechanism of the fractal dimension, the reason for instability in α calibrated by the Gauss-Newton method can be explained. Figure 2 illustrates the operational schematic diagram of this calibration method. By calculating the relationship between the inversion accuracy Q of mass concentration of a small sample and the fractal dimension α, the optimum value is obtained by using the Gauss-Newton method, and there is an optimum value for each small sample. Therefore, the fractal dimension obtained by this method only describes the shape characteristic of a small sample. Due to the differences in shape characteristics of small samples in different ranges of mass concentration, α attained by the Gauss-Newton method will be different for different small samples. Therefore, it is not accurate that

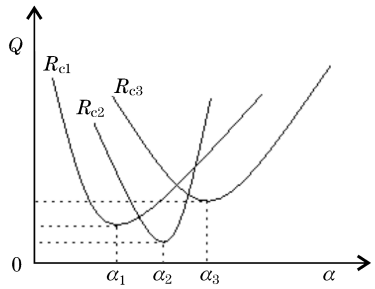

Fig. 2. Operational schematic diagram of α by the Gauss-Newton method.

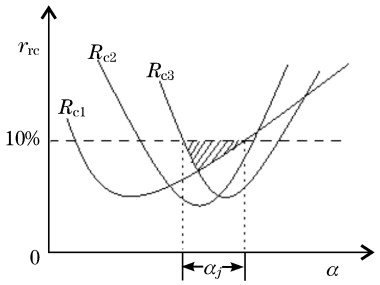

Fig. 3. Operational schematic diagram of α by the intersection point calibration method.

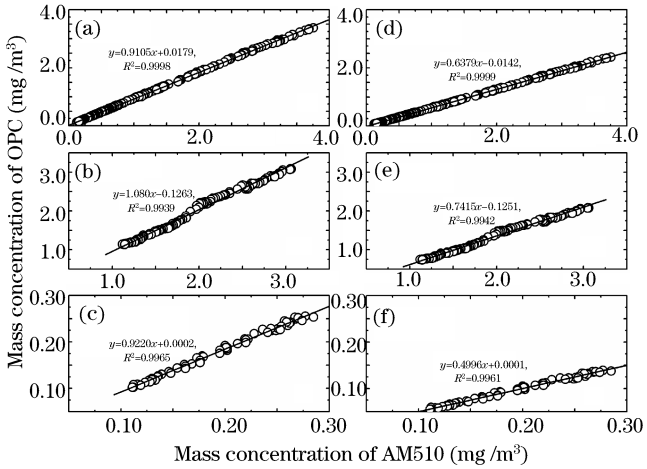

Fig. 4. Mass concentrations inversed by the model using calibration coefficients obtained by the intersection point calibration method versus mass concentrations measured by the SIDEPAK AM510 for (a) soot, (b) smoke, (c) air; mass concentrations obtained by the Gauss-Newton method versus those measured by AM510 for (d) soot, (e) smoke, (f) air.

the fractal dimension of a small sample obtained by the Gauss-Newton method is considered as the fractal dimension of the total measured particles.

Using the intersection point calibration method, the fractal dimension is obtained by calculating the intersection point of fractal dimensions of different small samples. This method satisfies the condition of the calibration mechanism that the common shape characteristic of different small samples is used to replace that of the measured particles. The operational schematic diagram of this calibration method is shown in Fig. 3, in which r_{TC} represents the relative error between inversed and actual mass concentrations, the fractal dimension α is attained by getting the average of the intersection α_j, and the detailed description of this method can be seen in Ref. [6].

To validate the intersection point calibration method which satisfies the condition of the calibration mechanism, it is used to detect aerosol mass concentration. We repeated the calibration experiments for 5 times, and the average of the five intersections α_j was taken as the fractal dimension α. The calibration sample is smoke, and then $\alpha = 0.435$ and $k = 3.014\times10^{-5}$ mg/m^3 are obtained for an OPC. For comparison, we also computed the calibration coefficients using the Gauss-Newton method, and $\alpha = 1.2065$, $k = 4.688\times10^{-5}$ mg/m^3 are attained by taking the average values of five calibration experiments. At last, we measured soot, smoke, and air, respectively. The pulse height distributions measured by the OPC combining α and k are applied to inverse mass concentrations, and the calculated values are compared with actual values C_{TSI}. Figures 4(a)−(c) illustrate the relationship of mass concentrations inversed by using the intersection point calibration method and measured by a norm-referenced instrument (TSI, SIDEPAK AM510 Aerosol Monitor), and the fitted equations and coefficient correlations are also shown in the figures. The slopes of the fitted lines are 0.9105, 1.080, and 0.9220, and the correlation coefficients are 0.9998, 0.9939, and 0.9965, respectively. Figures 4(d)−(f) illustrate the relationship between mass concentrations inversed by using the Gauss-Newton method and measured by the norm-referenced instrument. The slopes of the fitted lines are 0.6379, 0.7415, and 0.4996, and the correlation coefficients are 0.9999, 0.9942, and 0.9961, respectively. It can be seen that the slopes in Figs. 4(a)−(c) are all close to 1 and the experimental data are highly correlated, but the slopes in Figs. 4(d)−(f) are all much less than 1. The mass concentrations inversed by using the Gauss-Newton method are less than actual mass concentrations. Hence, we can come to a conclusion that the fractal dimension α obtained by the intersection point calibration method is accurate.

In conclusion, through discussing the stability of coefficients in our model for aerosol mass concentration, the concept of the fractal dimension of scattering equivalent section is put forward, which describes the shape characteristic of aerosol. Based upon this physical meaning and the viewpoint that the intersection point of the fractal dimension of different small samples is the optimum value of the fractal dimension of aerosols, the calibration mechanism of the fractal dimension is given. Theoretical analysis and experimental results indicate that the fractal dimension obtained according to this calibration mechanism is stable and precise. The investigation of the calibration mechanism for the fractal dimension of scattering equivalent section remarkably enhances the present model.

This work was supported by the Scientific Research Foundation of Nanjing University of Information Science & Technology under Grant No. 20080296.

References

1. Y. C. Chan, R. W. Simpson, G. H. McTainsh, P. D. Vowles, D. D. Cohen, and G. M. Bailey, Atmos. Environ. **31,** 3773 (1997).
2. M. Brauer, C. Avila-Casado, T. I. Fortoul, S. Vedal, B.

Stevens, and A. Churg, Environ. Health Perspect. **109,** 1039 (2001).
3. T. M. Peters, D. Ott, and P. T. O' Shaughnessy, Ann. Occup. Hyg. **50,** 843 (2006).
4. F. Gu, J. Yang, B. Bian, and A. He, Laser Technology (in Chinese) **31,** 360 (2007).
5. F. Gu, J. Yang, B. Bian, and A. He, Acta Opt. Sin. (in Chinese) **27,** 1706 (2007).
6. F. Gu, J. Yang, B. Bian, and A. He, Chin. Opt. Lett. **6,** 214 (2008).
7. F. Yan, H. Hu, and T. Yu, Chin. J. Quantum Electron. (in Chinese) **21,** 98 (2004).
8. A. Thomas and J. Gebhart, Atmos. Environ. **28,** 935 (1994).
9. D. E. Day, W. C. Malm, and S. M. Kreidenweis, J. Air Waste Manage. Assoc. **50,** 710 (2000).
10. J. S. Olfert, J. P. R. Symonds, and N. Collings, J. Aerosol Sci. **38,** 69 (2007).
11. P. Gwaze, O. Schmid, H. J. Annegarn, M. O. Andreae, J. Huth, and G. Helas, J. Aerosol Sci. **37,** 820 (2006).
12. J. P. R. Symonds, K. St. J. Reavell, J. S. Olfert, B. W. Campbell, and S. J. Swift, J. Aerosol Sci. **38,** 52 (2007).
13. F. J. Taguas, M. A. Martín, and E. Perfect, Geoderma **88,** 191 (1999).
14. A. Virtanen, J. Ristimäki, and J. Keskinen, Aerosol Sci. Technol. **38,** 437 (2004).